Inter-Tier Interference Coordination in Massive-MIMO System based on Statistical Channel Information

Rui Peng and Yafei Tian
School of Electronics and Information Engineering, Beihang University, Beijing, China
Email: pengrui@buaa.edu.cn, ytian@buaa.edu.cn

***Abstract*—We study the interference coordination in massive-MIMO heterogeneous network. In this scene, macro-users (MUEs) are distributed in clusters and pico-cells are separated from MUEs. There exists the inter-tier interference and it is hard to implement interference coordination since the instantaneous channel state information (CSI) between macro-base station (MBS) and pico-users (PUEs) is hard to obtain. In this circumstance, we propose a two-tier precoding method based on the statistical CSI between MBS and pico-base station (PBS) with the minimum mean square error (MMSE) criterion to form deeper nulling for pico-cells close to MBS. In our method, the outer precoder is designed to mitigate the inter-cluster and the inter-tier interference, and the inner precoder aims to suppress the intra-cluster interference. Simulation results show that our statistical CSI based on the MMSE precoding scheme could mitigate the inter-tier interference efficiently in channels with small spatial angular spread. The proposed method could achieve better throughput than other precoding methods for PUEs close to MBS.**

***Index Terms*—Heterogeneous network, massive-MIMO, MMSE, statistical CSI, two-tier precoding**

I. Introduction

Massive-MIMO and heterogeneous network are the key technologies in the fifth generation mobile communication system. Massive-MIMO possesses more degrees of freedom (DoF), providing higher array gain and diversity gain [1]. Moreover, the introduction of pico-cells enables users to get closer to the pico-base station (PBS), which may help to improve the signal-to-noise ratio (SNR) of users and meanwhile serve more users.

However, massive-MIMO heterogeneous network has some challenges. Firstly, the deployment of pico-cells introduces inter-tier interference where pico-users (PUEs) will suffer strong interference from macro-base station (MBS). Secondly, it is complicated for the MBS to achieve instantaneous channel state information (CSI) of each user. Therefore, an inter-tier interference coordination method with low complexity will meet the demand of massive-MIMO heterogeneous network.

Recently, some interference coordination schemes have been proposed to achieve higher user data rate. [2] proposed a precoding scheme to mitigate the strong inter-tier interference of offloaded users with full CSI, where MBS uses zero forcing (ZF) precoding to supress inter-tier interference and PBS uses max ratio transmission (MRT) precoding to serve the offloaded users. In this scheme, however, it is hard to obtain the instantaneous CSI from MBS to offloaded users. An enhanced inter-cell interference coordination (eICIC) method was introduced in LTE-Advanced [3], where MBS and PBS use different time slots to transmit the data. Although it could completely eliminate inter-tier interference, the spectral efficiency would be halved. [4] proposed a two-tier precoding method based on zero forcing block diagonalization (ZF-BD) criterion in the scene that macro users locate in clusters. Outer precoder uses statistical CSI to mitigate the inter-cluster interference and inner precoder uses effective instantaneous CSI to suppress the intra-cluster interference. On this base, [5] and [6] proposed "spatial blanking" scheme. In addition to the statistical information from MBS to macro-users (MUEs), this scheme further uses statistical information from MBS to PBS to mitigate the inter-tier interference through an outer precoder based on ZF criterion. This method could reduce the inter-tier interference to some extent, but with the growing number of pico-cells and MUEs, there would be no enough DoF in MBS to generate the null space. Besides, we hope to generate deeper beam nulling at positions that close to MBS, and generate shallower beam nulling at positions that far away from the MBS, since the pico-cells close to MBS will suffer stronger inter-tier interference.

In this work, we propose a two-tier precoding method based on the minimum mean square error (MMSE) criterion. Outer precoder utilizes the statistical CSI to mitigate the inter-cluster and the inter-tier interference while inner precoder uses the instantaneous effective channel information to reduce the intra-cluster interference. We demonstrate that the proposed two-tier MMSE precoder performs better than other precoding schemes and has greater advantage on the case that pico-cells is close to the MBS. Furthermore, we will analyze the impact of the spatial angular spread on the performance of our proposed method.

The paper is organized as follows: Section II describes the system model in detail. Section III introduces the algorithm of two-tier MMSE precoding including the outer precoder and the inner precoder. Section IV shows simulation and analysis results. Finally, conclusion will be made in Section V.

II. System Model

In the single cell heterogeneous network, we consider a macro-cell comprised of one MBS and multiple PBSs. MUEs

scatter in groups and PUEs distribute randomly in pico-cells. Considering that users either access to MBS or PBS according to their received SNR so MUEs cannot exist in the area of pico-cells, i.e., the pico-cells and MUEs are separated. The network layout is shown in Fig. 1.

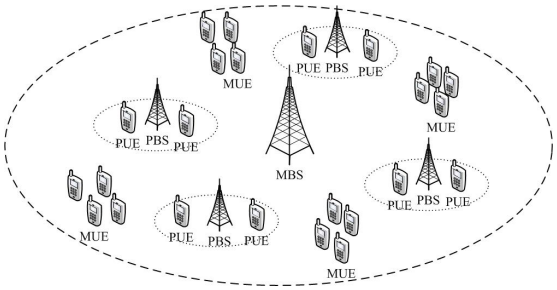

Fig. 1. Network layout of the considered heterogeneous network.

We assume that the MBS equips large scale antenna array with M_{macro} antennas and each PBS has M_{pico} antennas. All users have one antenna. There are N_{p} PBSs in the macro-cell. In this scene, MBS and PBS use the same frequency band. MUEs are divided into G clusters and each cluster has K_g users. Each PBS serves K_{p} PUEs. The noise power of user is denoted by P_N. The total transmit power of MBS and PBS are denoted by P_{macro} and P_{pico}. After normalization, the power become $P_{\text{m}} = P_{\text{macro}}/P_N$ and $P_{\text{p}} = P_{\text{pico}}/P_N$.

We suppose that the distance between PBS and MUE is long and the power of PBS is much lower than that of MBS, so we ignore the interference from PBSs to MUEs and the interference among pico-cells. In this case, the received signal of the k-th MUE in the g-th cluster is given by

$$y_{g_k} = \boldsymbol{h}_{g_k,\text{m}}\boldsymbol{v}_{g_k,\text{m}}x_{g_k,\text{m}} + \sum_{i\neq k}\boldsymbol{h}_{g_k,\text{m}}\boldsymbol{v}_{g_i,\text{m}}x_{g_i,\text{m}} + \sum_{j\neq g}\boldsymbol{h}_{g_k,\text{m}}\boldsymbol{V}_{j,\text{m}}\boldsymbol{x}_{j,\text{m}} + n_{g_k}, \quad (1)$$

where $\boldsymbol{h}_{g_k,\text{m}} \in \mathbb{C}^{1\times M_{\text{macro}}}$ is the channel vector between MBS and the k-th MUE in g-th cluster, $\boldsymbol{v}_{g_k,\text{m}} \in \mathbb{C}^{M_{\text{macro}}}$ is the precoding vector for this user. $\boldsymbol{V}_{g,\text{m}} = [\boldsymbol{v}_{g_1,\text{m}},\cdots,\boldsymbol{v}_{g_{K_g},\text{m}}]$ denotes the precoding matrix for the g-th cluster, $\boldsymbol{x}_{g,\text{m}} = [x_{g_1,\text{m}},\cdots,x_{g_{K_g},\text{m}}]^T$ is the data vector and $n_{g_k} \sim \mathcal{CN}(0,1)$ is the additive white Gaussian noise (AWGN). In (1), $\boldsymbol{h}_{g_k,\text{m}}\boldsymbol{v}_{g_k,\text{m}}x_{g_k,\text{m}}$ is the expected signal, $\sum_{i\neq k}\boldsymbol{h}_{g_k,\text{m}}\boldsymbol{v}_{g_i,\text{m}}x_{g_i,\text{m}}$ is the intra-cluster interference and $\sum_{j\neq g}\boldsymbol{h}_{g_k,\text{m}}\boldsymbol{V}_{j,\text{m}}\boldsymbol{x}_{j,\text{m}}$ is the inter-cluster interference.

Similarly, the received signal of the i-th PUE in each pico-cell is given by

$$y_i = \boldsymbol{h}_{i,\text{p}}\boldsymbol{v}_{i,\text{p}}x_{i,\text{p}} + \sum_{j\neq i}\boldsymbol{h}_{i,\text{p}}\boldsymbol{v}_{j,\text{p}}x_{j,\text{p}} + \boldsymbol{h}_{i\text{m}}\boldsymbol{V}_{\text{m}}\boldsymbol{X}_{\text{m}} + n_i, \quad (2)$$

where $\boldsymbol{h}_{i,\text{p}} \in \mathbb{C}^{1\times M_{\text{pico}}}$ is the channel vector between PBS and the i-th PUE, $\boldsymbol{v}_{i,\text{p}} \in \mathbb{C}^{M_{\text{pico}}}$ is the precoding vector for this PUE. $\boldsymbol{h}_{i\text{m}} \in \mathbb{C}^{1\times M_{\text{macro}}}$ denotes the channel vector between MBS and this PUE, $\boldsymbol{V}_{\text{m}} = [\boldsymbol{V}_{1,\text{m}},\cdots,\boldsymbol{V}_{G,\text{m}}]$ denotes the precoding matrix for all the MUEs, $\boldsymbol{X}_{\text{m}} = [\boldsymbol{x}_{1,\text{m}}^H,\cdots,\boldsymbol{x}_{G,\text{m}}^H]^H$ is the data vector of MUEs. In (2), $\boldsymbol{h}_{i,\text{p}}\boldsymbol{v}_{i,\text{p}}x_{i,\text{p}}$ is the expected signal for the PUE. $\sum_{j\neq i}\boldsymbol{h}_{i,\text{p}}\boldsymbol{v}_{j,\text{p}}x_{j,\text{p}}$ is the interference between PUEs in a pico-cell, $\boldsymbol{h}_{i\text{m}}\boldsymbol{V}_{\text{m}}\boldsymbol{X}_{\text{m}}$ is the interference from MBS.

Consider the scene that neighbor users share the same channel covariance matrix $\boldsymbol{R}_k$. According to Karhunen-Loeve representation [7], the channel vector between MBS and user is given as

$$\boldsymbol{h}_{k,\text{m}}^H = \boldsymbol{U}_k\boldsymbol{\Lambda}_k\boldsymbol{w}_k, \quad (3)$$

where $\boldsymbol{U}_k \in \mathbb{C}^{M_{\text{macro}}\times r}$ is the matrix of the eigenvectors corresponding to non-zero eigenvalues of $\boldsymbol{R}_k$, r is the rank of $\boldsymbol{R}_k$ and $\boldsymbol{\Lambda}_k \in \mathbb{C}^{r\times r}$ is an diagonal matrix whose elements are the nonzero eigenvalues of $\boldsymbol{w}_k \sim \mathcal{CN}(0,\boldsymbol{I}_r)$.

III. Two-tier MMSE Precoding

In heterogeneous network, PUEs are disturbed by the MBS, so we hope that precoding scheme in MBS could guarantee the sum data rate of MUEs and at the same time reduce the interference to PUEs. Without loss of generality, we suppose that users could only feedback the information to the base station which serves it. In other words, the instantaneous CSI between MBS and PUEs could not be estimated directly. Besides, due to the large quantity of antennas in massive-MIMO, estimating the instantaneous CSI leads to high complexity. Hence, we utilize a two-tier MMSE precoder in the MBS, where the outer precoder is designed through the statistical CSI to mitigate the inter-cluster and the inter-tier interference, also it will help to reduce the dimension of inner precoder.

In Section II, we had assumed that neighbor users share the same channel covariance matrix because they are quite close with nearly the same angle of departure. Thus the MUEs in one cluster will have the same statistical CSI. Similarly, the radius of pico-cell is much smaller than the distance from MBS to PBS, so the statistical CSI between MBS and PUE could be approximated by the statistical CSI between MBS and PBS.

The precoding matrix in the MBS is presented as

$$\boldsymbol{V}_{\text{m}} = \boldsymbol{A}\boldsymbol{D}, \quad (4)$$

where $\boldsymbol{A} \in \mathbb{C}^{M_{\text{macro}}\times K_gG}$ is the outer precoding matrix which aims to mitigate the inter-cluster interference and the inter-tier interference; $\boldsymbol{D} \in \mathbb{C}^{K_gG\times K_gG}$ is the inner precoding matrix which is used to reduce the intra-cluster interference in the effective channel.

A. Outer precoder

The outer precoder is based on the MMSE criterion. For one cluster of MUEs, the outer precoding matrix guarantees the channel gain of these MUEs and forms nulls at the positions of other clusters and pico-cells. We hope that the effective channel matrix after outer precoding is an approximate block diagonal matrix

$$\boldsymbol{H}_{\text{e}} = \begin{pmatrix} \boldsymbol{H}_{1,\text{m}}\boldsymbol{A}_1 & \boldsymbol{H}_{1,\text{m}}\boldsymbol{A}_2 & \cdots & \boldsymbol{H}_{1,\text{m}}\boldsymbol{A}_G \\ \boldsymbol{H}_{2,\text{m}}\boldsymbol{A}_1 & \boldsymbol{H}_{2,\text{m}}\boldsymbol{A}_2 & \cdots & \boldsymbol{H}_{2,\text{m}}\boldsymbol{A}_G \\ \vdots & \vdots & \ddots & \vdots \\ \boldsymbol{H}_{G,\text{m}}\boldsymbol{A}_1 & \boldsymbol{H}_{G,\text{m}}\boldsymbol{A}_2 & \cdots & \boldsymbol{H}_{G,\text{m}}\boldsymbol{A}_G \end{pmatrix} \quad (5)$$

where $\boldsymbol{A}_g \in \mathbb{C}^{M_{\text{macro}} \times K_g}$ is the outer precoder for the g-th cluster MUEs, $\boldsymbol{H}_{g,\text{m}} = [\boldsymbol{h}_{g_1,\text{m}}^H, \cdots, \boldsymbol{h}_{g_{K_g},\text{m}}^H]^H$ denotes the channel matrix between MBS and the g-th cluster. The diagonal matrix element $\boldsymbol{H}_{g,\text{m}}\boldsymbol{A}_g$ is the effective channel matrix for MUEs in cluster g. The off-diagonal element $\boldsymbol{H}_{g,\text{m}}\boldsymbol{A}_{g'}(g \neq g')$ is the effective inter-cluster interference channel. After outer precoding, the inter-cluster interference $\boldsymbol{H}_{g,\text{m}}\boldsymbol{A}_{g'} \approx \boldsymbol{0}$ and the inter-tier interference $\boldsymbol{h}_{i\text{m}}\boldsymbol{A}_g \approx \boldsymbol{0}$.

The design of outer precoding matrix is described in detail in the following. Assume that $\boldsymbol{R}_{g,\text{m}} = E[\boldsymbol{H}_{g,\text{m}}^H \boldsymbol{H}_{g,\text{m}}]$ is the statistical channel covariance matrix for the g-th cluster. In FDD system, users estimate this statistical CSI in a period of time and feed back it to MBS. In TDD system, the MBS estimates the downlink CSI by the pilots in uplink due to the channel reciprocity. $\boldsymbol{R}_{j,\text{p}} = E[\boldsymbol{H}_{p_j,\text{m}}^H \boldsymbol{H}_{p_j,\text{m}}]$ is the statistical channel covariance matrix for the j-th pico-cell, which could be calculated by PBSs and then fed back to the MBS through backhual link. $\boldsymbol{R}_g$ is the weighted sum of the channel covariance matrix of interference clusters and pico-cells,

$$\boldsymbol{R}_g = \sum_j w_j \boldsymbol{R}_{j,\text{p}} + \sum_{i \neq g} \boldsymbol{R}_{i,\text{m}}. \tag{6}$$

In (6), we find that for the pico-cells close to MBS, $\boldsymbol{R}_{j,\text{p}}$ will be larger, so the outer precoder could form deeper nulls at the positions of these pico-cells. Moreover, to adjust the interference to each pico-cell, we introduce a weighting factor w_j. If we expect to form a deeper null at the position of pico-cell j, we can give a larger w_j to improve the proportion of $\boldsymbol{R}_{j,\text{p}}$ in $\boldsymbol{R}_g$. In practice, the PUE feedbacks channel quality index (CQI) to the PBS periodically, thus the PBS can estimate the inter-tier interference power and report to the MBS through the X2 interface. Based on some fairness rules, the MBS can dynamically adjust the weighting factors to control the interference levels to each pico-cell. Due to limited space, the fairness rule and the dynamical adjustment algorithm are not discussed in detail in this paper.

According to the MMSE criterion, the precoding matrix

$$\boldsymbol{V}_{g,\text{MMSE}} = (\boldsymbol{H}^H\boldsymbol{H} + \alpha\boldsymbol{I})^{-1}\boldsymbol{H}_g^H, \tag{7}$$

where $\boldsymbol{H} = [\boldsymbol{H}_{1,\text{m}}^H, \cdots, \boldsymbol{H}_{G,\text{m}}^H, \boldsymbol{h}_{1\text{m}}^H, \cdots, \boldsymbol{h}_{K_\text{p}\text{m}}^H]^H$ is the collection of all the channel vectors between the MBS and all users. α is the diagonal loading factor, which controls the trade-off between the interference mitigation and the expected signal gain. Thus we have

$$\boldsymbol{V}_{g,\text{MMSE}}\boldsymbol{V}_{g,\text{MMSE}}^H = (\boldsymbol{H}^H\boldsymbol{H}+\alpha\boldsymbol{I})^{-1}\boldsymbol{H}_g^H\boldsymbol{H}_g(\boldsymbol{H}^H\boldsymbol{H}+\alpha\boldsymbol{I})^{-1} \tag{8}$$

Substituting the statistical CSI instead of the instantaneous CSI. We get

$$\boldsymbol{V}_{g,\text{MMSE}}\boldsymbol{V}_{g,\text{MMSE}}^H = (\boldsymbol{R}_g + \alpha\boldsymbol{I})^{-1}\boldsymbol{R}_{g,\text{m}}(\boldsymbol{R}_g + \alpha\boldsymbol{I})^{-1}. \tag{9}$$

When α is small, the capability to mitigate the inter-tier interference will be strong, while the beam gain to the expected users will be decreased. In this paper, we select a compromised value $\alpha = G/P_\text{m}$ [8].

The outer precoding matrix $\boldsymbol{A}_g$ for group g is finally obtained by choosing the eigenvectors of $\boldsymbol{V}_{g,\text{MMSE}}\boldsymbol{V}_{g,\text{MMSE}}^H$ corresponding to its largest K_g eigenvalues. Thus the whole outer precoding matrix is

$$\boldsymbol{A} = [\boldsymbol{A}_1, \boldsymbol{A}_2, \cdots, \boldsymbol{A}_G]. \tag{10}$$

B. Inner precoder

After outer precoding, the inter-tier interference and the inter-cluster interference would be greatly reduced. Furthermore, the dimension of the effective channel is shrunk, which is helpful to acquire the instantaneous effective CSI. Inner precoder is used to deal with the intra-cluster interference. We use RZFBF-PGP (regularized zero forcing per-group processing) for the inner precoding matrix [4]. In this case, MBS treats each group separately, so we only need to estimate and feed back diagonal matrix elements $\boldsymbol{H}_{g,\text{m}}\boldsymbol{A}_g$ in the effective channel $\boldsymbol{H}_\text{e}$ instead of the whole matrix. The inner precoding matrix for group g is calculated as

$$\boldsymbol{D}_g = (\boldsymbol{H}_{g,\text{e}}^H\boldsymbol{H}_{g,\text{e}} + a\boldsymbol{I})^{-1}\boldsymbol{H}_{g,\text{e}}^H, \tag{11}$$

where $\boldsymbol{H}_{g,\text{e}} = \boldsymbol{H}_{g,\text{m}}\boldsymbol{A}_g$ is the effective channel for cluster g, and $a = K_g G/P_\text{m}$.

The precoding matrix takes on the block-diagonal form of

$$\boldsymbol{D} = \xi \cdot \text{diag}(\boldsymbol{D}_1, \cdots, \boldsymbol{D}_G), \tag{12}$$

where ξ is normalizing parameter. To satisfy the power constraint

$$\text{trace}(\xi^2\boldsymbol{D}^H\boldsymbol{A}^H\boldsymbol{A}\boldsymbol{D}) = P_\text{m}, \tag{13}$$

we have

$$\xi = \sqrt{P_\text{m}/\text{trace}(\boldsymbol{D}^H\boldsymbol{A}^H\boldsymbol{A}\boldsymbol{D})}. \tag{14}$$

IV. Simulation Results

In this section, we evaluate the performance of the two-tier MMSE precoding method. MBS antennas are arranged in uniform planar array. We specify that the direction of normal line of the antenna plane is 0 degree in horizonal and 90 degree in vertical. Setting the position of MBS as the coordinate origin, the MUEs and PBSs are distributed in 3D space with that the azimuth angle ranges from -60 to 60 degrees and the zenith angle ranges from 45 to 135 degrees. The radius of pico-cells is proportional to the distance from the PBS to the MBS. This requirement follows the actual cell selection procedure. Since users usually access to base station which provides stronger received power, so the pico-cells close to the MBS will have a shorter radius. Assume that PUEs are located in the edge of pico-cells. In this circumstance, each PUE has nearly the same received signal power from PBS and MBS.

Considering the urban scenario, we use the 3GPP 3D channel model [9] to compare the performance of different precoding methods and study the impact of spatial angular spread. In the 3GPP 3D channel model, electromagnetic waves go through reflection and scattering. A transmit beam is divided into several cluster beams, and each cluster has multi-path rays with different angles of departure.

A. Beam pattern

To demonstrate the property that the two-tier MMSE precoder will form deeper nulls at the positions of pico-cells close to the MBS, we first compare the beam pattern of two-tier MMSE and spatial blanking precoders in 3D-MIMO channels. In this simulation, we deploy one group MUEs and 3 pico-cells. The location parameters are shown in Table I. To calculate the pattern, we traverse all the angles in 3D space and generate the normalized channel vector $\boldsymbol{h}(\theta,\phi)$. The gain of each point is calculated as

$$\boldsymbol{A}(\theta,\phi) = \text{trace}\left(\boldsymbol{h}(\theta,\phi)\boldsymbol{V}_{\text{m}}\boldsymbol{V}_{\text{m}}^{H}\boldsymbol{h}(\theta,\phi)^{H}\right), \quad (15)$$

and the obtained beam patterns are shown in Fig. 2(a) and Fig. 2(b).

TABLE I
LOCATION PARAMETERS

MUE	
Azimuth angle	0-5 degree
Zenith angle	135 degree
Distance to MBS	210m-280m
PBS	
Azimuth angle	30,-30,-60 degree
Zenith angle	90 degree
Distance to MBS	50m,150m,450m

We can find that the two-tier MMSE precoding method has deeper beam nulls at the location of all pico-cells than that formed by the spatial blanking method. Besides, among the 3 beam nulls formed by two-tier MMSE, the depth is inversely proportional to the distance between the pico-cell and the MBS, while for the spatial blanking method, beam null depth is not relevant to the distance. Therefore, the two-tier MMSE method has better interference suppression capability, especially for the pico-cells close to the MBS.

B. Performance with different distance from PBS to MBS

To give a more comprehensive analysis of the performance of the two-tier MMSE, we observe the average interference to noise ratio (INR) and the sum data rate of PUEs with different distances from the PBS to the MBS. We compare with three precoding schemes: two-tier MMSE, ZF-BD and spatial blanking. In this simulation, assume that all PBSs have the same noise power and the same distance to MBS, which ranges from 50m to 500m. Since the transmit power is normalized by the noise power, the INR of PUE i is given by

$$\text{INR}_i = \boldsymbol{h}_{i\text{m}}\boldsymbol{V}_{\text{m}}\boldsymbol{V}_{\text{m}}^{H}\boldsymbol{h}_{i\text{m}}^{H}. \quad (16)$$

Because PBS uses ZF precoding to serve multiple users, there will be no interference between PUEs. The data rate of the i-th PUE is calculated as in (17). The simulation results are shown in Fig. 3 and Fig. 4, and the simulation parameters are listed in Table II.

TABLE II
SIMULATION PARAMETERS

Setting scenario	Value
Macro cell radius	500m
Center frequency	2GHz
Number of PBS	8
Number of cluster	4
MUEs in per cluster	4
PUEs in per pico-cell	4
Simulation type	Monte-Carlo
Number of samples	1000
Setting MBS	
Transmit power	46dBm
Noise power	SNR 5dB for the cell-edge users
Antenna spacing	$\lambda/2$
Number of antennas	128(16 horizon 8 verticle)
Channel model	3D MIMO channel
Precoder scheme	Two-tier MMSE
Setting PBS	
Transmit power	30dBm
Distance from PBS to MBS	50m-500m
Pico-cell radius	7.92m-71.32m
Number of antennas	4
Channel model	Rayleigh channel
Precoder scheme	Zero forcing

$$C_{i,\text{p}} = \log\left|1 + \frac{\boldsymbol{h}_{i,\text{p}}\boldsymbol{v}_{i,\text{p}}\boldsymbol{v}_{i,\text{p}}^{H}\boldsymbol{h}_{i,\text{p}}^{H}}{\boldsymbol{h}_{i\text{m}}\boldsymbol{V}_{\text{m}}\boldsymbol{V}_{\text{m}}^{H}\boldsymbol{h}_{i\text{m}}^{H}+1}\right|. \quad (17)$$

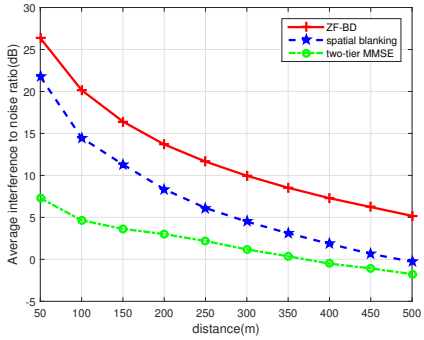

Fig. 3. Average INR of PUEs with different distance from the PBS to MBS.

Fig. 3 shows that for ZF-BD precoding scheme, PUEs suffer strong inter-tier interference since there is no inter-tier interference coordination. The spatial blanking could reduce the inter-tier interference with about 5dB, but for the PUEs close to MBS, the inter-tier interference still has strong power. The two-tier MMSE precoding could reduce the interference with about 15-20dB for the pico-cells near MBS. For pico-cells far away from MBS, the two-tier MMSE scheme still

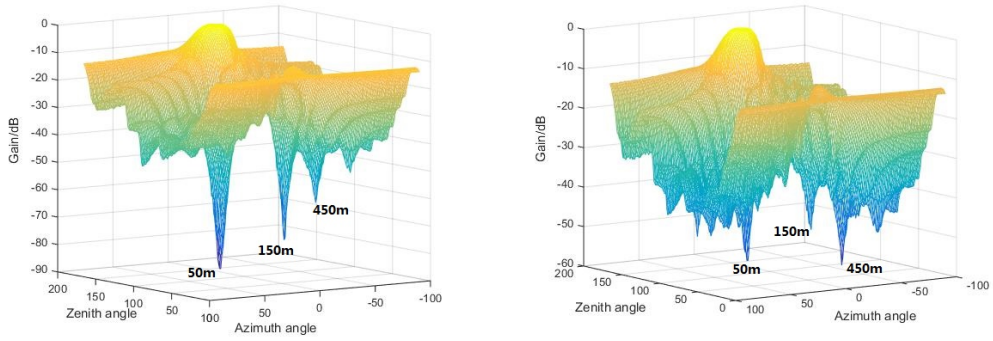

(a) (b)

Fig. 2. (a) Two-tier MMSE beam pattern, (b) Spatial blanking beam pattern.

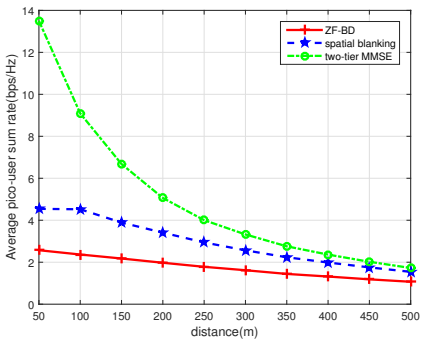

Fig. 4. Average sum rate of PUEs with different distance from the PBS to MBS.

has the lowest inter-tier interference power, although the gap is narrower.

In Fig. 4, the trend is consistent with that in Fig. 3, the two-tier MMSE has superior average sum rate performance. For pico-cells at the distance of 50 m, the two-tier MMSE scheme has 3 times average user data rate than that achieved by spatial blanking.

C. Cumulative distribution function of user data rate

In this part, we compare the achieved data rate of MUEs and PUEs of three inter-tier interference coordination methods, i.e., two-tier MMSE, spatial blanking and eICIC. The data rate of the k-th MUE in the g-th group is calculated as in (18). The cumulative distribution function (CDF) curves for data rate of MUEs and PUEs are shown in Fig. 5.

Fig. 5(a) and Fig. 5(b) prove that the two-tier MMSE scheme has better performance than spatial blanking and eICIC for improving the PUE data rate. In the pico-cells close to the MBS, two-tier MMSE scheme has higher average data rate and less low data rate users than spatial blanking and eICIC schemes. In the pico-cells far away from the MBS, the two-tier MMSE is still superior to the other two precoding methods but the advantage is not that bigger. Fig. 5(c) shows that, on the data rate of MUEs, the two-tier MMSE has similar performance with the spatial blanking. Among the three precoding methods, eICIC is worst. Although eICIC has no inter-tier interference, the time resource utilization is only half of that in two-tier MMSE and spatial blanking, which degrades the user data rate dramatically.

D. Compare statistical CSI with perfect CSI

In this part, we compare the two-tier MMSE precoding method based on statistical CSI with ZF and MMSE precoding methods based on perfect instantaneous CSI. To show the impact of statistical CSI, channels with different spatial angular spread of the rays are simulated. With the growth of angular spread, the channel correlation in the cluster will decline, and the correlation among the clusters will increase. In addition, the rank of the channel covariance matrix $\boldsymbol{R}_k$ will be higher with larger angular spread.

The average sum rates of MUEs are shown in Fig. 6(a), where the MMSE precoding with perfect instantaneous CSI has the best performance. We can see that, when the angular spread is small, the two-tier MMSE with statistical CSI has a similar performance. But with the increase of angular spread, the performance gap is enlarged. For PUEs, Fig. 6(b) shows that the average sum rate of two-tier MMSE rises initially and then falls with the angular spread increasing. This nonmonotonic trend can be explained by the following two reasons. On one hand, since there exists angle deviation between PUEs and PBSs, when the angular spread is very small, the statistical CSI from MBS to PUE could not be completely replaced by the statistical CSI from MBS to PBS. On the other hand, when the angular spread is large, the difference between the statistical CSI and the instantaneous CSI will be expanded, so the performance will degrade as well.

V. Conclusion

In this paper, we proposed a two-tier MMSE precoding scheme in massive-MIMO heterogeneous network. The outer precoder aims to reduce the inter-cluster and the inter-tier interference, and the inner precoder is proposed to suppress the residual intra-cluster interference. Although the statistical CSI between the MBS and the PBS is used, the inter-tier interference can still be suppressed effectively. With the MMSE criterion, we can form deeper beam nulls at the positions of pico-cells close to the MBS, and the throughput of these pico-cells can be significantly improved. Simulation results show

$$C_{g_k,m} = \log\left|1 + \frac{\boldsymbol{h}_{g_k,m}\boldsymbol{v}_{g_k,m}\boldsymbol{v}_{g_k,m}^H\boldsymbol{h}_{g_k,m}^H}{\sum_{i\neq k}\boldsymbol{h}_{g_k,m}\boldsymbol{v}_{g_i,m}\boldsymbol{v}_{g_i,m}^H\boldsymbol{h}_{g_k,m}^H + \sum_{j\neq g}\boldsymbol{h}_{g_k,m}\boldsymbol{V}_{j,m}\boldsymbol{V}_{j,m}^H\boldsymbol{h}_{g_k,m}^H + 1}\right|. \quad (18)$$

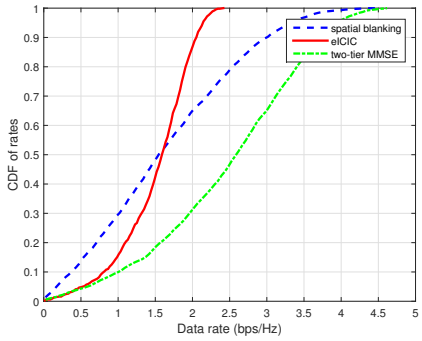

(a)

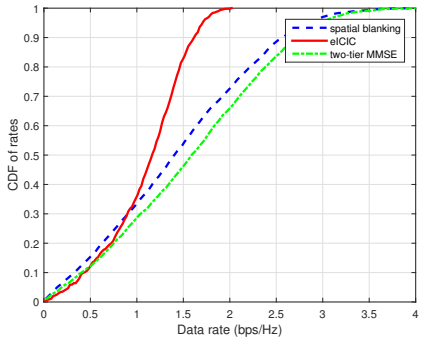

(b)

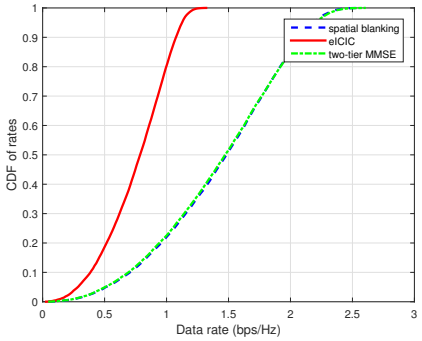

(c)

Fig. 5. (a) CDF of PUE data rate in pico-cells with distance of 100m to MBS, (b) CDF of PUE data rate in pico-cells with distance of 450m to MBS, (c) CDF of MUE data rate.

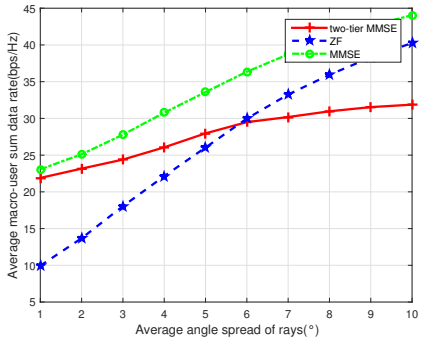

(a)

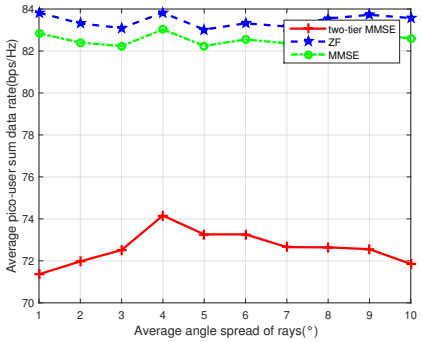

(b)

Fig. 6. (a) The sum rate of MUEs with different angular spread, (b) The sum rate of PUEs with different angular spread

that the two-tier MMSE scheme has better performance than other interference coordination methods, and can works well in channels with small spatial angular spread.

ACKNOWLEDGEMENTS

This work was supported by the National Natural Science Foundation of China under Grant 61371077, and the National High Technology Research and Development Program of China under Grant 2014AA01A703.

REFERENCES

[1] E. Larsson, O. Edfors, F. Tufvesson, and T. Marzetta, "Massive-MIMO for next generation wireless systems," *IEEE Commun. Mag.*, vol. 52, pp. 186–195, Feb. 2014.

[2] Y. Wu, Y. Cui, and B. Clerckx, "Analysis and optimization of inter-tier interference coordination in downlink multi-antenna HetNets with offloading," *IEEE Transactions on Wireless Communications*, vol. 14, pp. 6550–6564, Dec. 2015.

[3] D.Lopez-Perez, I. Guvenc, G. de la Roche, M. Kountouris, T. Q. S. Quek, and J. Zhang, "Enhanced intercell interference coordination challenges in heterogeneous networks," *IEEE Wireless Communications 2011*, vol. 18, pp. 22–30, Jun. 2011.

[4] A. Adhikary, J. Nam, J. Ahn, and G. Caire, "Joint spatial division and multiplexing: The large-scale array regime," *IEEE Trans. Inf. Theory*, vol. 59, pp. 6441–6463, Oct. 2013.

[5] A. Adhikary, E. A. Safadi, and G. Caire, "Massive-MIMO and inter-tier interference coordination," in *ITA 2014*, 2014, pp. 1–10.

[6] A. Adhikary, H. S. Dhillon, and G. Caire, "Massive-MIMO meets HetNet: Interference coordination through spatial blanking," *IEEE J. Select. Areas Communications*, vol. 33, pp. 1171–1186, Jun. 2015.

[7] A. Adhikary, E. A. Safadi, M. Samimi, R. Wang, G. Caire, T. S. Rappaport, and A. F. Molisch, "Joint spatial division and multiplexing for mm-wave channels," *IEEE J. Select Areas Communications*, vol. 32, pp. 1239–1255, Jun. 2014.

[8] C. B. Peel, B. M. Hochwald, and A. L. Swindlehurst, "A vector-perturbation technique for near-capacity multiantenna multiuser communication-Part I: Channel inversion and regularization," *IEEE Trans. Communications*, vol. 59, pp. 195–202, Jan. 2005.

[9] *3GPP TR 36.873, V12.0.0, Rel. 12*, Sep. 2014.